

# Towards Exascale Lattice Boltzmann computing

S. Succi<sup>1,2,5</sup>, G. Amati<sup>3</sup>, M. Bernaschi<sup>5</sup>, G. Falcucci<sup>4,2</sup>, M.  
Lauricella<sup>5</sup>, and A. Montessori<sup>5</sup>

<sup>1</sup>Italian Institute of Technology, Center for Life Nanoscience at La  
Sapienza, 00161, Rome, Italy

<sup>2</sup>John A. Paulson School of Engineering and Applied Sciences,  
Harvard University, 33 Oxford St., 02138 Cambridge, MA, USA

<sup>3</sup>SCAI, SuperComputing Applications and Innovation Department,  
CINECA, Via dei Tizii, 6, 00185 Rome, Italy

<sup>4</sup>Department of Enterprise Engineering “Mario Lucertini”,  
University of Rome Tor Vergata, Via del Politecnico 1, 00133  
Rome, Italy

<sup>5</sup>Istituto per le Applicazioni del Calcolo CNR, Via dei Taurini 19,  
00185 Rome, Italy

January 15, 2022

# Contents

<b>1</b>	<b>Introduction</b>	<b>5</b>
<b>2</b>	<b>Basic Lattice Boltzmann Method</b>	<b>7</b>
2.1	The stream-collide LB paradigm . . . . .	9
<b>3</b>	<b>Improving LB performance</b>	<b>11</b>
3.1	Data storage and allocation . . . . .	11
3.2	Fusing Stream-Collide . . . . .	13
3.3	Hiding communication costs . . . . .	14
<b>4</b>	<b>Petascale and the roadmap to Exascale computers</b>	<b>15</b>
4.1	Vanilla LB: back of envelope calculations . . . . .	18
4.2	Present-day Petascale LB application . . . . .	19
<b>5</b>	<b>Tentative ideas</b>	<b>21</b>
5.1	Time-delayed LB . . . . .	22
5.2	Fault-tolerant LB . . . . .	23
5.2.1	Check-Point Restart protocols . . . . .	23
5.2.2	Mitigating Silent Data Corruptions . . . . .	26
<b>6</b>	<b>Prospective Exascale LB applications</b>	<b>27</b>

## List of Figures

1	D3Q27 lattice, composed of a set of 27 discrete velocities (left). D3Q19 lattice, composed of a set of 19 discrete velocities (right).	29
2	Roofline Model obtained for an intel Phi processor: for $F/B < 10$ the effective processing speed grows linearly with $F/B$ , whereas for $F/B > 10$ it comes to a saturation, dictated by the raw processing rate. Increasing $F/B$ much beyond, does not win any additional performance. The vertical line indicates the performance range for a "Vanilla Lattice Boltzmann". . . . .	30
3	Vorticity and velocity contour for the flow around a cylinder . . .	31
4	Vorticity for a "clean" cylinder (top) and a "decorated" one (bottom).	36
5	Strong scaling for a $512^3$ gridpoint simulation. Note the superlinear speed-up achieved up to 128 nodes (i.e. 512 task). . . . .	37
6	Weak scaling using $128^3$ gridpoint per task. Using 2744 tasks (686 nodes) 84% of parallel efficiency is obtained. . . . .	38
7	Different configurations of emulsions. In panel (a) the continuous to dispersed flow rate ratio $Q_d^{in}/(2Q_c^{in}) = 2$ whereas in panel (b) is set to one. The viscosities (in lattice unit) are the same for the two fluids and set to $\nu = 0.0167$ and the velocities of the two fluids at the inlet channels are (in lattice units/step) (a): $u_d^{in} = 0.01$ , $u_c^{in} = 0.01$ , (b): $u_d^{in} = 0.01$ , $u_c^{in} = 0.005$ . . . . .	39

## Abstract

We discuss the state of art of Lattice Boltzmann (LB) computing, with special focus on prospective LB schemes capable of meeting the forthcoming Exascale challenge. After reviewing the basic notions of LB computing, we discuss current techniques to improve the performance of LB codes on parallel machines and illustrate selected leading-edge applications in the Petascale range. Finally, we put forward a few ideas on how to improve the communication/computation overlap in current large-scale LB simulations, as well as possible strategies towards fault-tolerant LB schemes.

## 1 Introduction

Exascale computing refers to computing systems capable of delivering Exaflops, one billion billions ( $10^{18}$ , also known as *quintillion*) floating-point operations per second, that is one floating-point operation every billionth of a billionth of second, also known as Attosecond ( $10^{-18}$  s). Just to convey the idea, at Attosecond resolution, one can take a thousand snapshots of an electron migrating from one atom to another to establish a new chemical bond. Interestingly, the attosecond is also the frontier of current day atomic clock precision, which means clocks that lose or gain less than two seconds over the entire age of the Universe!

In 2009 Exascale was projected to occur in 2018, a prediction which turned out to be fulfilled just months ago, with the announcement of a 999 PF/s sustained

throughput computational using the SUMMIT supercomputer [1]<sup>1</sup>. Mind-boggling as they are, what do these numbers imply for the actual advancement of science? The typical list includes new fancy materials, direct simulation of biological organs, fully-digital design of cars and airplanes with no need of building physical prototypes, a major boost in cancer research, to name but a few.

Attaining Exaflop performance on each of these applications, however, is still an open challenge, because it requires a virtually perfect match between the system architecture and the algorithmic formulation of the mathematical problem.

In this article, we shall address the above issues with specific reference to a class of mathematical models known as Lattice Boltzmann (LB) methods, namely a lattice formulation of Boltzmann's kinetic equation which has found widespread use across a broad range of problems involving complex states of flowing matter [2]. The article is organized as follows: in Section 2 we briefly introduce the basic features of the LB method. In Section 3 the state-of-the-art of LB performance implementation will be briefly presented, whereas in Section 4 the main aspects of future exascale computing are discussed, along with performance figures for current LB schemes on present-day Petascale machines. Finally, in Section 5 we sketch out a few *tentative* ideas which may facilitate the migration of LB codes to Exascale platforms.

---

<sup>1</sup>This figure was obtained using half precision (FP16) floating point arithmetic.

## 2 Basic Lattice Boltzmann Method

The LB method was developed in the late 1980's as a noise-free replacement of lattice gas cellular automata for fluid dynamic simulations [2].

Ever since, it has featured a (literal) exponential growth of applications across a remarkably broad spectrum of complex flow problems, from fully developed turbulence to micro and nanofluidics [3], all the way down to quark-gluon plasmas [4, 5].

The main idea is to solve a minimal Boltzmann kinetic equation for a set of discrete distribution functions (*populations* in LB jargon)  $f_i(\vec{x}; t)$ , expressing the probability of finding a particle at position  $\vec{x}$  and time  $t$ , with a (discrete) velocity  $\vec{v} = \vec{c}_i$ . The set of discrete velocities must be chosen in such a way as to secure enough symmetry to comply with mass-momentum-energy conservation laws of macroscopic hydrodynamics, as well as with rotational symmetry. Figure 1 shows two of the 3D lattices most widely used for current LB simulations, with a set of 19 discrete velocities (D3Q19) or 27 velocities (D3Q27).

In its simplest and most compact form, the LB equation reads as follows:

$$f(\vec{x} + \vec{c}_i, t + 1) = f'_i(\vec{x}; t) \equiv (1 - \omega)f_i(\vec{x}; t) + \omega f_i^{eq}(\vec{x}; t) + S_i, \quad i = 0, b \quad (1)$$

where  $\vec{x}$  and  $\vec{c}_i$  are 3D vectors in ordinary space,  $f_i^{eq}$  is the equilibrium distribution function and the lattice time step is made unit, so that  $\vec{c}_i$  is the length of the link connecting a generic lattice site node  $\vec{x}$  to its  $b$  neighbors,  $\vec{x}_i = \vec{x} + \vec{c}_i$ .

In the above, the local equilibria are provided by a lattice truncation, to second

order in the Mach number  $M = u/c_s$ , of the Maxwell-Boltzmann distribution, namely

$$f_i^{eq}(\vec{x}; t) = w_i \rho (1 + u_i + q_i) \quad (2)$$

where  $w_i$  is a set of weights normalized to unity,  $u_i = \frac{\vec{u} \cdot \vec{c}_i}{c_s^2}$  and  $q_i = u_i - u^2/D$ , in  $D$  spatial dimensions.

Finally,  $S_i$  is a source term encoding the fluid interaction with external (or internal) sources, the latter being crucial to describe multiphase flows with potential energy interactions.

The above equation represents the following situation: the populations at site  $\vec{x}$  at time  $t$  collide to produce a post-collisional state  $f'_i(\vec{x}; t)$ , which is then scattered away to the corresponding neighbors at  $\vec{x}_i$  at time  $t + 1$ . Provided the lattice is endowed with suitable symmetries, and the local equilibria are chosen accordingly, the above scheme can be shown to reproduce the Navier-Stokes equations for an isothermal quasi-incompressible fluid of density and velocity

$$\rho = \sum_i f_i \quad \vec{u} = (\sum_i f_i \vec{c}_i) / \rho \quad (3)$$

The relaxation parameter  $\omega$  dictates the viscosity of the lattice fluid according to

$$\nu = c_s^2 (\omega^{-1} - 1/2) \quad (4)$$

Full details can be found in the vast literature on the subject [6][7].



## 2.1 The stream-collide LB paradigm

The main strength of the LB scheme is the stream-collide paradigm, which stands in marked contrast with the advection-diffusion of the macroscopic representation of fluid flows.

Unlike advection, streaming proceeds along straight lines defined by the discrete velocities  $\vec{c}_i$ , regardless of the complexity of the fluid flow. This is a major advantage over material transport taking place along fluid lines, whose tangent is given by the fluid velocity itself, a highly dynamic and heterogeneous field in most complex flows. To be noted that streaming is literally exact. i.e., there is no round-off error, as it implies a memory shift only with no floating-point operation.

For the case of a 2D lattice, discounting boundary conditions, the streaming along positive and negative  $v_x$  ( $p=1, 2$ ) can be coded as shown in Algorithms 2.1 and 2.2.

Note that the second loop runs against the flow, i.e. counterstream, so as to avoid overwriting memory locations, which would result in advancing the same population across the entire lattice in a single time step! A similar trick applies to all other populations: the  $(i, j, k)$  loops must run counter the direction of propagation.

This choice makes possible to work with just a single array for time levels  $t$  and  $t + 1$ , thereby halving the memory requirements.

With this streaming in place, one computes the local equilibria distribution  $f_i^{eq}$  as a quadratic combination of the populations and moves on to the collision step, as shown in pseudocode 2.3. This completes the inner computational engine of

LB. In this paper, we shall not deal with boundary conditions, even though, like with any computational fluid-dynamic method, they ultimately decide the quality of the simulation results. We highlight only that the exact streaming permits to handle fairly complex boundary conditions in a *conceptually* transparent way [9] because information always moves along the straight lines defined by the discrete velocities. Actual programming can be laborious, though.

---

**Algorithm 2.1:** IN-PLACE STREAMING  $v_x > 0(.)$

```

for  $j \leftarrow 1$  to  $ny$ 
for  $i \leftarrow 1$  to  $nx$ 
 $f(1, i, j) = f(1, i - 1, j)$ 

```

---

**Algorithm 2.2:** IN-PLACE STREAMING  $v_x < 0(.)$

```

for  $j \leftarrow 1$  to  $ny$ 
for  $i \leftarrow nx$  to  $1$ 
 $f(2, i, j) = f(2, i + 1, j)$ 

```

---

**Algorithm 2.3:** COLLISION STEP(.)

```

for  $j \leftarrow 1$  to  $ny$ 
for  $i \leftarrow 1$  to  $nx$ 
for  $p \leftarrow 1$  to  $npop$ 
 $f(p, i, j) = (1 - \omega) * f(p, i, j, k) + \omega * f^{eq}(p, i, j)$ 

```

### 3 Improving LB performance

The LB literature provides several “tricks” to accelerate the execution of the basic LB algorithms above described. Here we shall briefly describe three major ones, related to optimal data storage and access, as well as parallel performance optimisation.

#### 3.1 Data storage and allocation

The Stream-Collide paradigm is very powerful, but due to the comparatively large number of discrete velocities, it shows exposure to memory bandwidth issues, i.e. the number of bytes to be moved to advance the state of each lattice site from time  $t$  to  $t+1$ . Such data access issues have always been high on the agenda of efficient LB implementations, but with prospective Exascale LB computing in mind, they become vital.

Thus, one must focus on efficient data allocation and access practices. There are two main and mutually conflicting ways of storing LB populations (assuming row-major memory order as in C or C++ languages):

- By contiguously storing the set of populations living in the same lattice site:

`fpop[nx][ny][npop]` (AoS, Array of Structures)

- By contiguously storing homologue streamers across the lattice:

`fpop[npop][nx][ny]` (SoA, Structure of Arrays)

The former scenario, AoS, is optimal for collisions since the collision step requires

no information from neighbouring populations and it is also cache-friendly, as it presents unit stride access, i.e., memory locations are accessed contiguously, with no jumps in-between.

However, AoS is non-optimal for streaming, whose stride is now equal to  $n_{pop}$ , the number of populations.

The latter scenario, SoA, is just reciprocal, i.e., optimal for streaming, since it features a unitary stride, but inefficient for collisions, because it requires  $n_{pop}$  different streams of data at the same time.

These issues are only going to get worse as more demanding applications are faced, such multiphase or multicomponent flows requiring more populations per lattice site and often also denser stencils. Whence the need of developing new strategies for optimal data storage and access. A reliable performance estimate is not simple, as it depends on a number of hardware platform parameters, primarily the latency and bandwidth of the different levels of memory hierarchy.

An interesting strategy has been presented by Aniruddha and coworkers [11], who proposed a compromising data organization, called AoSoA. Instead of storing all populations on site, they propose to store only relevant subsets, namely the populations sharing the same energy (energy-shell organization). For instance, for the D3Q27 lattice, this would amount to four energy shells: energy 0 (just 1 population), energy 1 (6 populations), energy 2 (12 populations) and energy 3 (8 populations). This is sub-optimal for collisions but relieves much strain from streaming. As a matter of fact, by further ingenious sub-partitioning of the energy shells, the authors manage to capture the best of the two, resulting in an execution

of both Collision and Streaming at their quasi-optimal performance.

Note that in large-scale applications, streaming can take up to 30 per cent of the execution time even though it does not involve any floating-point operation!

In [10] a thorough analysis of various data allocation policies is presented.

### 3.2 Fusing Stream-Collide

Memory access may take a significant toll if stream and collide are kept as separate steps (routines). Indeed, node-wise, using a single-phase double precision D3Q19 LB scheme, there are  $19 \times 8 \times 2 = 304$  bytes involved in memory operations (load/store) per  $\simeq 250$  Flops of computation, corresponding to a rough computation to memory ratio of  $\simeq 0.7$  Flops/Byte.

The memory access issue was recognized since the early days of LB implementations and led to the so-called fused, or push, scheme. In the fused scheme (eq. 5), streaming is, so to say, “eaten up” by collisions and replaced by non-local collisions [12].

$$f'(p, i, j, k; t + 1) = (1 - \omega) * f(p, ip, jp, kp; t) + \omega * f^{eq}(p, ip, jp, kp; t) \quad (5)$$

where  $(ip, jp, kp)$  is the pointee of site  $(i, j, k)$  along the  $p$ -th direction. As one can appreciate, the streaming has virtually disappeared, to be embedded within non-local collisions, at the price of doubling memory requirements (two separate arrays at  $t$  and  $t + 1$  are needed) and a more complex load/store operation.

Actually, fused versions with a *single* memory level have also appeared in the lit-

erature, but it is not clear whether their benefits are worth the major programming complications they entail [13]. Moreover the chance of executing them in parallel mode is much more limited.

### 3.3 Hiding communication costs

The third major item, which is absolutely crucial for multiscale applications, where LB is coupled to various forms of particle methods, is the capability of hiding the communication costs by overlapping communication and calculation when running in parallel mode. Technically, this is achieved by using non-blocking communication send/receive MPI primitives as shown in pseudo-algorithm 3.1:

---

**Algorithm 3.1:** NON-BLOCKING RECEIVE(.)

*SourceTask(st) : Send(B, dt)*

*SourceTask(st) : Do\_some\_work()*

*DestinationTask(dt) : Receive(B, st)*

where  $B$  is the boundary data to be transferred from source to destination, in order for the latter to perform its chunk of computation. The send operation is usually non-blocking, i.e. the source task keeps doing other work while the memory subsystem is transmitting the data, because these data are, so to say, not its concern. The destination task, on the other hand, cannot start the calculation until those data are received, hence the safe procedure is to sit idle until those data are actually received, i.e. the blocking-receive scenario.

However, if other work, not contingent to the reception of those data is available,

there is obviously no point of waiting, whence the point of non-blocking receive. In other words, after posting its request for data from another task, the given task proceeds with the calculations which are free from causal dependencies on the requested data, until it is notified that these data are finally available.

This is of course way more complicated than just sitting idle until the requested data arrive, as it requires a detailed command at the concurrent timeline of the parallel code. However, non-blocking receive operations are absolutely key: without hiding communication costs, multiscale LB applications would not get any near to the extreme performance they have attained in the last decade. As an example, the multiscale code MUPHY [14] scaled from tens of Teraflops in 2011 to 20 Petaflops in 2013, providing a precious asset for the design of future exascale LB code.

A description of the state of the art of HPC LB can be found in [15].

## **4 Petascale and the roadmap to Exascale computers**

Back in 1975, Gordon Moore predicted doubling of computing power every 18 months, namely a thousandfold increase every fifteen years [16]. A unique case in the history of technology, such prediction, now going by the name of Moore's law, has proved correct for the last four decades, taking from CRAY's Megaflops of the early 80's to the current two hundreds Petaflops of Summit supercomputer [17].

Besides decreasing single-processor clock time, crucial to this achievement has

proven the ability of supercomputer architectures to support concurrent execution of multiple tasks in parallel.

The current leading entries in the list of top-500 performers support up to millions of such concurrent tasks and each CPU hosts tens of basic computing units, known as “cores”. The promised 2020’s Exascale machine will cater to hundreds of million of cores, with a core-clock still in the GHz range, because of heat power constraints. As a consequence, an Exascale code should be prepared to exploit up to *a billion* concurrent cores, each of them able to perform billions of floating point operations:  $10^{18} = 10^9 \times 10^9$ . This “symmetry” between computation and number of units that need to communicate reflects and mandates a perfect balance between the two.

Indeed, as performance ramps up, it is increasingly apparent that accessing data could become more expensive than make computations using them: *Bytes/s* is taking over *Flops/s* as a metrics for extreme performance.

Besides hardware issues, Exascale computing also bears far-reaching implications on computational science, setting a strong premium on algorithms with low data traffic, low I/O, lean communication to computation ratios and high fault-tolerance. The point is simple, but worth a few additional comments.

Let  $F$  being the number of Flops required by a given application,  $B$  the corresponding number of Bytes,  $\dot{F}$  the processing speed (Flops/s) and  $\dot{B}$  (Bytes/s) the corresponding bandwidth. On the assumption of no overlap between memory ac-



cess and computation, the execution time is given by the sum of the two, namely:

$$t = \frac{F}{\dot{F}} + \frac{B}{\dot{B}} \quad (6)$$

The corresponding effective processing rate is given by:

$$\dot{F}_{eff} \equiv F/t = \frac{\dot{F}}{1 + \phi} \quad (7)$$

where

$$\phi \equiv \frac{\dot{F}/\dot{B}}{F/B} \quad (8)$$

This shows that in order to attain the peak performance  $\dot{F}$ , corresponding to no data access overheads (infinite bandwidth), one must secure the condition  $\phi \ll 1$ . Indeed, for  $\phi \ll 1$ , i.e., a “large”  $F/B$ , we have  $\dot{F}_{eff} \sim \dot{F}$ , whereas in the opposite limit  $\phi \gg 1$ , a “small”  $F/B$ , the effective processing rate flattens at  $\dot{F}_{eff} \sim (F/B) \dot{B}$ , i.e., a fraction of the bandwidth. This is a (simplified) version of the so-called roofline model [18].

In a symbolic form, the roofline condition (8) can be written as “*Flops/Bytes much larger than (Flops/s)/(Bytes/s)*”. The former depends solely on the application, whereas the latter is dictated by the hardware instead.

The “threshold” value, at which the transition between memory-bound to floating-point-bound regimes occurs, is, for present hardware (fig. 6),  $F/B \sim 10$ .

## 4.1 Vanilla LB: back of envelope calculations

Using a simple *Vanilla* LB (VLB), i.e. single-phase, single time relaxation, 3D lattice with fused collision, the roofline model permits to estimate limiting figures of performance. In Fig. 6 the roofline for an Intel phi is shown<sup>2</sup>.

The technical name of the ratio between flops and data that need to be loaded/stored from/to memory is Operational Intensity, OI for short, but we prefer to stick to our  $F/B$  notation to keep communication costs in explicit sight.

It provides information about code limitations: whether it is bandwidth-bound ( $F/B < 10$ ) or floating-point bound ( $F/B > 10$ ), as shown in Fig. 6. The HPL code used to rank supercomputers [17] is floating-point bound<sup>3</sup>.

For a VLB,  $F \simeq 200 \div 250$  is the number of floating point operations per lattice site and time step and  $B = 19 * 2 * 8 = 304$  is load/store demand in bytes, using double precision, hence  $F/B \sim 0.7$ , which spells “bandwidth-bound”. Boundary conditions operations are not considered here, for the sake of simplicity.

Memory Bandwidth in current-day hardware, at single node level, is about  $\simeq 400$  GB/s for an Intel Xeon Phi 7250 using MCDRAM in flat mode. MCDRAM is faster than RAM memory but it is limited in size (16 GB). It can be used as a further cache level (cache mode) or auxiliary memory (flat mode) [19].

For a “standard server” like Intel Xeon Platinum 8160 server Memory Bandwidth is  $\simeq 150$  GB/s.

According to technological trends, bandwidth is not expected to exceed 500 GB/s

---

<sup>2</sup>Bandwidth and Float point computation limits are obtained performing *stream* e HPL benchmark

<sup>3</sup>All hardware is built to exploit performance for floating point bound codes.

by 2020 [20]. Using as LB performance metrics GLUPS (Giga Lattice Update Per Second), due to the fact that LB is memory bounded the peak value is 400 GB/s, the limit is  $400(GB/s)/305(B/LUPS)$  yielding 1.3 GLUPS for a Phi node, so that the ratio  $\dot{F}/\dot{B} \sim 5$ , yielding an overhead factor  $\phi \sim 5/0.7 \sim 7$ : the effective processing speed is  $\dot{F}_{eff} \sim 0.125\dot{F}$ .

For an Exascale machine with order of  $10^5$  nodes and 500 GB/s Bandwidth per node, a peak of  $\sim 2 \times 10^{14}$  LUPS is expected.

## 4.2 Present-day Petascale LB application

As a concrete example of current-day competitive LB performance, we discuss the case of the flow around a cylinder (Fig. 3, 4): the goal is to study the effect on vorticity reduction using *decorated* cylinders [21] . To describe short-scale decorations, such as those found in nature, resolutions in the Exascale range are demanded since the simulation can easily entail six spatial decades (meters to microns).

Clearly, more sophisticated techniques, such as grid-refinement [22], or unstructured grids, could significantly reduce the computational demand, but we shall not delve into these matters here.

Indeed, if the “simple” computational kernel is not performing well on today Petascale machines, there is no reason to expect it would scale up successfully to the Exascale.

Hence, we next discuss performance data for a Petascale class machine (Marconi, Intel Phi based [23]) for a VLB code. Starting from the performance of a VLB, a

rough estimate of more complex LB's can be provided: a Shan-Chen multiphase flow [24], essentially two coupled VLB's, is about 2-3 times slower than VLB. Our VLB code reached about 0.5 GLUPs for a single node, equivalent to about 50% of the theoretical peak according to the roofline models<sup>4</sup>.

In Fig. 6 the strong scaling is presented for a  $512^3$  resolution, One point must be underlined: super-linear performance is due to the MCDRAM Memory limitation. Below four nodes, memory falls short of storing the full problem, hence a slower standard RAM is instead used. The best performance per node ( $\simeq 500GLUPs$ ) is reached for a size of about  $256^3$  per node, using 4 tasks and 17 threads per node. In Fig. 6 weak scaling results are presented using  $128^3$  gridpoints per task, 4 task per node, 17 threads per task. A reasonably good performance, a parallel efficiency of 84% is obtained using up to 700 nodes, that means a 1.4 PFlops peak performance.

Three different levels of *parallelism* have to be deployed for an efficient Exascale simulation:

- At core/floating point unit level: (e.g., using vectorization)
- At node level: (i.e., shared memory parallelization with threads)
- At clustRoofKNL.jpeger level: (i.e., distributed memory parallelization with task)

The user must be able to manage all the three levels but the third one depends

---

<sup>4</sup>The nodes are Phi in cache mode, which means about 300 GB/s, hence an upper limit of about 1 GLUPS

not only by the user (Sec. 3.3), since the performance crucially depends on the technology and the topology of the network, as well as on the efficiency of the communication software.

## **5 Tentative ideas**

It is often argued that Exascale computing requires a new computational “ecosystem”, meaning by this that hardware, software and computational algorithms, must all work in orchestrated harmony.

The challenges associated with achieving the above task on exascale machines is likely to require an optimal balance between evolutionary versus revolutionary changes to the existing algorithms, as well as to the programming models. For very informative discussions on these topics, see [30, 31, 32]. Besides scalability, the authors point out a number of additional crucial metrics, such as resilience to failure rates and silent errors, energy-consumption, runtime reconfigurability, as well as new programming models and languages aimed at supporting the above metrics. In the following, we present some potentially new ideas on the specific topics of communication/computation overlap and fault-tolerance in prospective exascale LB applications.

## 5.1 Time-delayed LB

The idea of time-delayed PDE's as a means of further hiding communication costs has been recently put forward by Ansumali and collaborators [25]. The main point is to apply the Liouvillean operator  $L$  at a delayed past time  $t - \tau$ , namely:

$$\partial_t f(t) = Lf(t - \tau) \quad (9)$$

A formal Taylor expansion shows that this is tantamount to advancing the system at time  $t$  via a retarded Liouvillean  $L_\tau = Le^{-\tau L}$ .

The delay provides a longer lapse between the posting of data request (non-blocking send/receive) and the actual reception, thereby leaving more time for doing additional work, while waiting for the requested data. In the case of LB, a M-level delayed streaming would look like follows

$$f_i(\vec{x}, t + 1) = \sum_{m=0}^M w_m f_i(\vec{x} - m\vec{c}_i, t - m) \quad (10)$$

where  $w_m$  are suitable normalized weights.

Incidentally, we note that for a negative-definite  $L$ , as required by stability,  $L_\tau$  is a dilatation of  $L$  for any  $\tau > 0$ . Therefore, besides introducing extra higher-order errors, the delayed scheme is subject to more stringent stability constraints than the standard one-time level version.

Nevertheless, once these issues are properly in place, delayed versions of LB might prove very beneficial for Exascale implementations.

## 5.2 Fault-tolerant LB

Another crucial issue in the Exascale agenda is to equip the computational model with error-recovery procedures, assisting the standard hardware operation against fault occurrences and silent errors (so far, hardware took up the full job).

Due to the large number of nodes/core, HW faults are very likely to appear routinely by a mere statistical argument [31]. As a consequence, not only at system level all libraries & API (e.g., MPI) have to be robust and fault-tolerant, but also the computational scheme.

To the best of our knowledge, for the case of LB, this key issue is entirely unexplored at the time of this writing.

### 5.2.1 Check-Point Restart protocols

The standard strategy to recover from system failures is Check-Point Restart (CPR), i.e. roll the system back to the closest checkpoint and resume execution from there. The CPR strategy is error-free, but very costly, since it requires a periodic dump of the full system configuration, easily in the order of tens of thousands trillions variables for Exascale applications (say, a cube of linear size  $10^5$  lattice units).

The frequency at which CPR must take place is strictly related to the expected failure rate of the system, which is a pretty complex quantity to assess. How-

ever, at a failure rate of about two per hour, as recently predicted on for exascale platforms[32], an exaflops/s LB simulation with  $10^{15}$  lattice sites, each taking  $10^3$  flops/site/step, would advance one timestep per second, which means about 1 CPR every 2000 steps. Although this is well separated from the simulation timescale, it places nonetheless a major strain on the I/O subsystem, as we are talking of the order of 1 Exabyte for each CPR.

A less-conservative but more sustainable procedure, consists of injecting a correction term at the time when the error is first detected and keep going from there, without any roll-back, a strategy sometimes referred to as *imprecise computing*.

The close-eyes hope is that a suitable correction term can be extrapolated from the past, and that the error still left shows capable of self-healing within a reasonably short transient time.

The first question is: how should such correction term look like?

Here comes a tentative idea.

Let  $t_{CP}$  be the time of most recent check-point and  $t_{ED}$  the time of error-detection (ED). One could estimate the reconstructed ED state by time-extrapolating from  $f(t_{CP})$  to  $f(t_{ED})$ . Formally

$$f^*(t_{ED}) = \mathcal{P}f(t_{CP}, t_1 \dots t_M) \quad (11)$$



where  $\mathcal{P}$  denotes some suitable Predictor operator, extrapolating from  $t_{CP}$  to  $t_{ED}$ . This assumes the availability of a sequence of outputs  $f(t_m)$ , where  $t_1 < t_2 \dots t_M < t_{CP}$ . Generally, that sequence is available but restricted to a set of hydrodynamic fields, say  $h$  for short, such as density and fluid velocity, namely four fields instead of twenty or so, major savings. Density and velocity are sufficient to reconstruct the equilibrium component  $f^{eq}$  but not the full distribution  $f = f^{eq} + f^{neq}$ , because the non-equilibrium component depends on the gradients (in principle at all orders) of the equilibrium. One could then partially reconstruct  $f^{neq}$  by taking first order gradients of density and velocity, a procedure which is going particularly touchy near the boundaries. Here a peculiar feature of LB may prove pretty helpful: the first order gradients do not need to be computed since they are contained in the momentum flux tensor, defined as  $\Pi = \sum_i f_i \vec{c}_i \vec{c}_i$ , a *local* combination of the populations.

If the momentum flux tensor is also stored in the hydrodynamic set  $h = \{\rho, \vec{u}, \Pi\}$ , then the first-order gradient contribution to non-equilibrium is already accounted for, and only higher order non equilibrium terms, usually called “ghosts” in LB jargon, are left out from the reconstruction. This is very good news; yet, it does not come for free, since the momentum flux tensor involves another six fields, for a total of ten, only half of the memory required by the full  $f$  configuration.

Regardless of which policy is used, the entire procedure hangs on the (reasonable?) hope that leaving ghosts out of the reconstruction of  $f(t_m)$ , is not going to compromise the quality of the predicted state  $f^*(t_{ED})$ .

Although only direct experimentation can tell, one may argue that numerical

methods equipped with inherent stability properties, such as the entropic LB [26], should stand good chances for fault-tolerant implementations. For instance, restricting the predicted solution to feature an entropy increase (or non-decrease) as compared to the current state at time  $t$ , may help improve the quality of the reconstruction procedure.

It should also be pointed out that higher-order moments can also be systematically reconstructed by suitable recursive procedures exploiting the recurrence relations between Hermite basis functions [27].

### **5.2.2 Mitigating Silent Data Corruptions**

The above procedures may prove pretty useful not only to design better CPR protocols, but also to mitigate the effects of silent errors, or better said, silent data corruptions (SDC's). SDC's are expected to become a major source of concern on exascale systems for a series of reasons, primarily the reduction in size and corresponding increase in number of elementary components, which enhances their exposure to, say, cosmic radiation. A number of studies show that although the majority of SDC's leads to explicit crashes, a smaller fraction corrupts the results without crashing the application, which is of course way more dangerous [32]. To the best of our knowledge, the vulnerability of LB to SDC's stands completely unexplored at the time of this writing. Here again, entropic formulations and/or recursive reconstruction of kinetic moments may offer new possibilities. For instance, some errors might remain silent. i.e. escape detection, at the level of lowest order moments but not at the ghost level, so that ghosts could be used as

SDC’s detectors.

Summarizing, the kinetic LB representation may offer new physics-inspired data-compression and error-detection/correction strategies to deal with fault-tolerance and silent data corruptions: the exploration of these strategies makes a very interesting research topic for the design of a new generation Exascale LB schemes.

## **6 Prospective Exascale LB applications**

In the present paper, we have discussed at length the challenges faced by LB to meet with Exascale requirements. Given that, as we hope we have been able to show, this is not going to be a plain “analytic continuation of current LB’s”, the obvious question before concluding is: what can we do once Exascale LB is with us? The applications are indeed many and most exciting.

For instance, Exascale LB codes will enable direct numerical simulations at Reynolds numbers around  $10^5 \div 10^6$ , thereby relieving much work from turbulence models. The full-scale design of automobiles will become possible.

At moderate Reynolds regimes, Exascale hemodynamics will permit to simulate a full heartbeat at red-blood cell resolution in about half an hour, thus disclosing new opportunities for precision medicine.

Likewise, Exascale LB-particle codes will allow millisecond simulations of protein dynamics within the cell, thereby unravelling invaluable information on many-body hydrodynamic effects under crowded conditions, which are vital to many essential biological functions, hence potentially also for medical therapies against

neurological diseases [28].

Further applications can be envisaged in micro-nanofluidics, such as the simulation of foams and emulsions at near-molecular resolution, so as to provide a much more detailed account of near-contact interface interactions, which are essential to understand the complex rheology of such flows. For instance, the macroscale structure (say mm) of soft-flowing crystals, i.e., ordered collections of liquid droplets within a liquid solvent (say oil in water), is highly sensitive to the nanoscale interactions which take place as interfaces come in near-contact, thereby configuring a highly challenging multiscale problem spanning six spatial decades and nearly twice as many in time [34].

As a very short example, Fig.6 shows different configurations of monodispersed emulsions at the outlet of the flow-focuser obtained by changing the dispersed/continuous flow rate ratios.

Such multiscale problem is currently handled via a combination of coarse-graining and grid-refinement techniques [29]. Exascale computing would drastically relax the need for both, if not lift it altogether, thereby paving the way to the computational design of mesoscale materials (mm) at near-molecular resolution (nm) [8]. The prospects look bright and exciting, but a new generation of ideas and LB codes are needed to turn this mind-boggling potential into a solid reality.

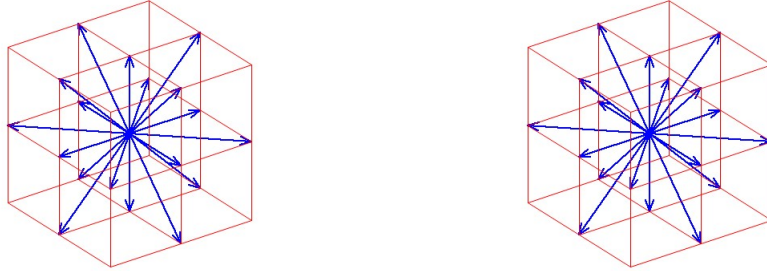


Figure 1: D3Q27 lattice, composed of a set of 27 discrete velocities (left). D3Q19 lattice, composed of a set of 19 discrete velocities (right).

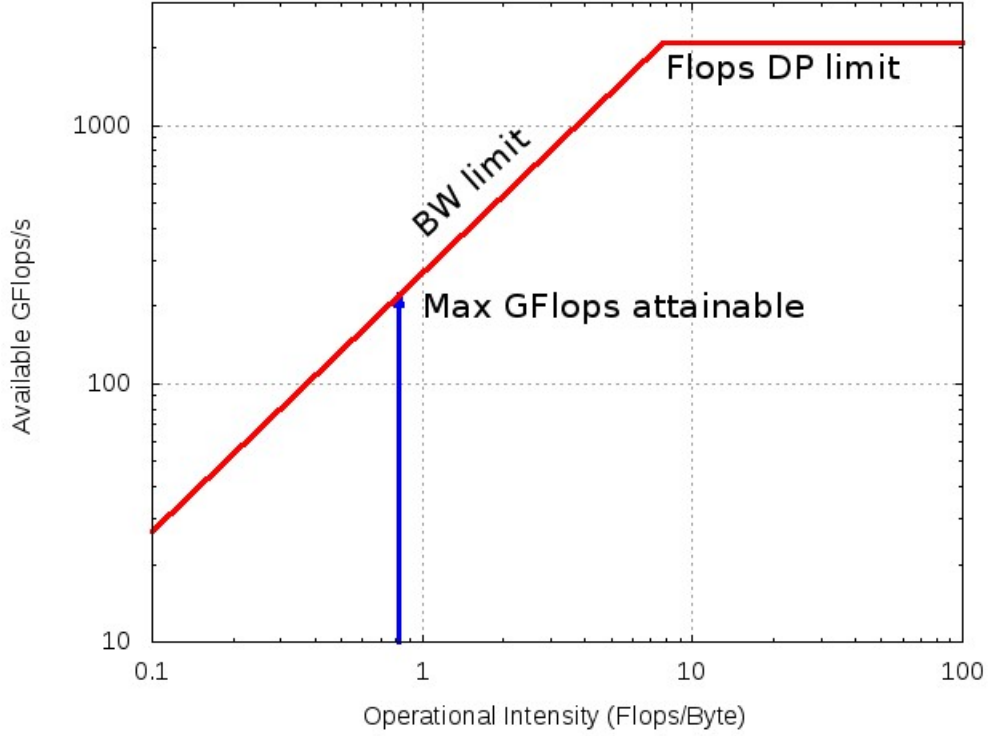


Figure 2: Roofline Model obtained for an intel Phi processor: for  $F/B < 10$  the effective processing speed grows linearly with  $F/B$ , whereas for  $F/B > 10$  it comes to a saturation, dictated by the raw processing rate. Increasing  $F/B$  much beyond, does not win any additional performance. The vertical line indicates the performance range for a "Vanilla Lattice Boltzmann".

## References

- [1] T. Kurth, S. Treichler et al, Exascale Deep Learning for Climate Analytics  
<https://arxiv.org/abs/1810.01993> (2018).
- [2] S. Succi, The Lattice Boltzmann Equation - For Complex States of Flowing  
 Matter, Oxford University Press, (2018).

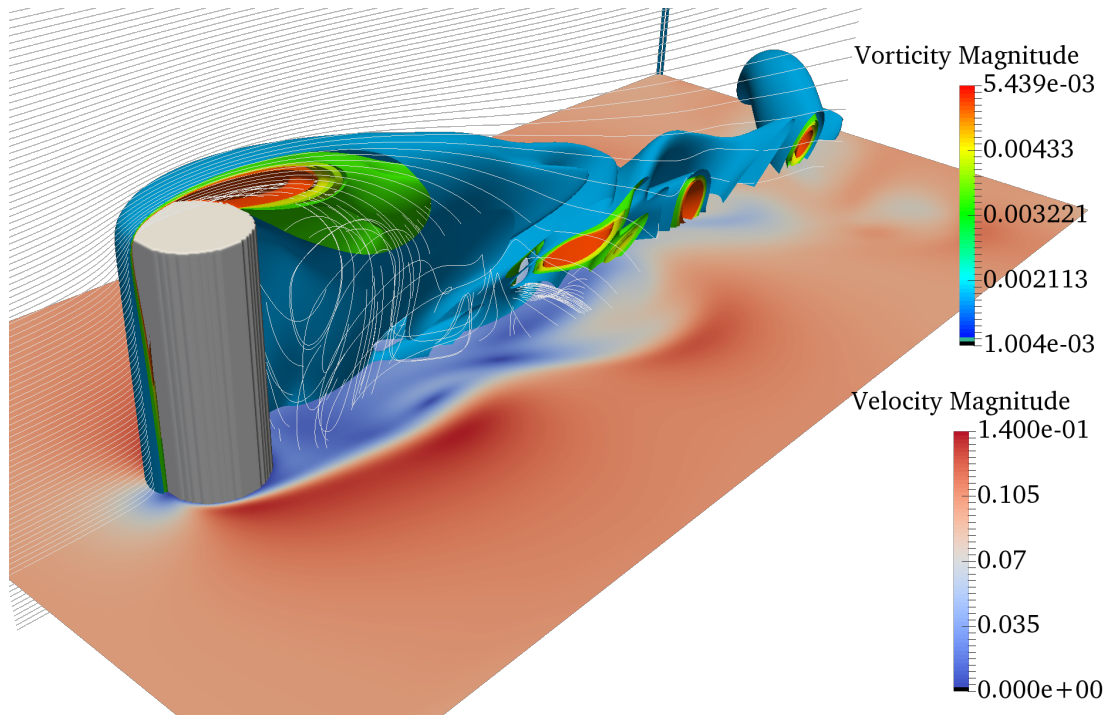


Figure 3: Vorticity and velocity contour for the flow around a cylinder

- [3] A. Montessori, P. Prestininzi et al., Lattice Boltzmann approach for complex nonequilibrium flows, Phys. Rev. E 92 (4), 043308 (2015)
- [4] S Succi, The European Physical Journal B 64 (3-4), 471-479 74 (2008)
- [5] S. Succi, Lattice Boltzmann 2038. EPL, 109 50001 (2015)
- [6] T. Kruger, H. Kusumaatmaja et al., The Lattice Boltzmann Method Principles and Practice, Springer (2017)
- [7] A. Montessori, G. Falcucci, Lattice Boltzmann Modeling of Complex Flows for Engineering Applications Morgan & Claypool Publishers, (2018)

- [8] A. Montessori, M. Lauricella et al., Elucidating the mechanism of step emulsification, *Phys. Rev. Fluids* 3, 072202(R) (2018)
- [9] S. Chen and D. Martnez, On boundary conditions in lattice Boltzmann methods *Physics of Fluids* 8, 2527 (1996)
- [10] IM.Wittmann, V.Haag at al., LBM Lattice Boltzmann benchmark kernels as a testbed for performance analysis, *Computers & Fluids* Volume 172, Pages 582-592 (2018)
- [11] G. S. Aniruddha, K. Siddarth et al., On vectorization of lattice based simulation, *Int. J. of Modern Physics C* Vol. 24, No. 12, 1340011 (2013)
- [12] K. Mattila, J. Hyvluoma et al., Comparison of implementations of the lattice-Boltzmann method, *Computers & Math. with Applications*, Vol. 55, 7, Pp 1514-1524 (2008)
- [13] F. Massaioli, G. Amati, Achieving high performance in a LBM code using OpenMP, The 4th European Workshop on OpenMP ([http://www.compunity.org/events/pastevents/ewomp2002/EWOMP02-09-1\\_massaioli\\_amati\\_paper.pdf](http://www.compunity.org/events/pastevents/ewomp2002/EWOMP02-09-1_massaioli_amati_paper.pdf)) (2002)
- [14] M. Bernaschi, S. Melchionna et al., MUPHY: A parallel MUlti PHYsics/scale code for high performance bio-fluidic simulations, *Comp. Phys. Comm.*, Vol. 180, 9, pp. 1495-1502, (2009)



- [15] F. Schornbaum, U. Rde: Massively Parallel Algorithms for the Lattice Boltzmann Method on Nonuniform Grids, SIAM Journal on Scientific Computing, 38(2): 96-126, 2016
- [16] G. E. Moore, Progress in digital integrated electronics, Electron Devices Meeting (1975)
- [17] <https://www.top500.org/>
- [18] S. Williams, A. Waterman et al., Roofline: an insightful visual performance model for multicore architectures, Communications of the ACM, Vol. 52, 4, pp.65-76, (2009)
- [19] A. Sodani, R. Gramunt et al., Knights Landing: Second-Generation Intel Xeon Phi Product, IEEE Micro, Vol. 36, 2 (2016)
- [20] J. D. McCalpin, Memory Bandwidth and System Balance in HPC systems, <http://sites.utexas.edu/jdm4372/2016/11/22/sc16-invited-talk-memory-bandwidth-and-system-balance-in-hpc-systems/>.
- [21] VK. Krastev, G. Amati, et al. On the effects of surface corrugation on the hydrodynamic performance of cylindrical rigid structures, Eur. Phys. J. E 41: 95 (2018)
- [22] D. Lagrava, O. Malaspinas et al., Advances in multi-domain lattice Boltzmann grid refinement, J. of Comput. Physics, Volume 231, 14, Pp 4808-4822 (2012)

- [23] <http://www.hpc.cineca.it/hardware/marconi>
- [24] X. Shan, H. Chen, Lattice Boltzmann model for simulating flows with multiple phases and components, *Phys. Rev. E* 47, 1815, (1993)
- [25] D. Mudigere, S. D. Sherlekar, et al., Delayed Difference Scheme for Large Scale Scientific Simulations *Phys. Rev. Lett.* 113, 218701 (2014)
- [26] S. Chikatamarla, S. Ansumali, et al., Entropic Lattice Boltzmann Models for Hydrodynamics in Three Dimensions, *Phys. Rev. Lett.* 97, 010201 (2006)
- [27] Coreixas C , Wissocq G , et al. Recursive regularization step for high-order lattice Boltzmann methods, *Phys. Rev. E*, 96,033306 (2017).
- [28] M. Bernaschi, S. Melchionna et al., Mesoscopic simulations at the physics-chemistry-biology interface. *Rev. Mod. Phys.*, 91(2), 025004 (2019).
- [29] A. Montessori et al, Mesoscale modelling of soft flowing crystals, *Phil. Trans. A*, Accepted, DOI 10.1098/rsta.2018.0149, 2018
- [30] Da Costa, Fahringer, et al., Exascale machines require new programming paradigms and runtimes, *Supercomputing frontiers and innovations*, 2, 6-27, (2015).
- [31] F. Cappello, A. Geist, W. Gropp et al, Towards Exascale Resilience, *Int. J. High Perform. Comput. Appl.*, 23(4), 374, (2014).
- [32] M. Snir, R.W. Wisniewski, J. A. Abraham et al, Addressing failures in exascale computing, *Int. J. High Perform. Comput. Appl.*, 28(2) 129, (2014).

- [33] P.L. Guhur, E. Constantinescu, D. Ghosh et al, Detection of Silent Data Corruption in Adaptive Numerical Integration Solvers, IEEE International Conference on Cluster Computing (CLUSTER). IEEE, 592, (2017).
- [34] A. Montessori, M. Lauricella and S. Succi, Mesoscale modelling of soft-flowing crystals, Phil. Trans. Roy. Soc. A, 377(2142), 20180149, (2019).

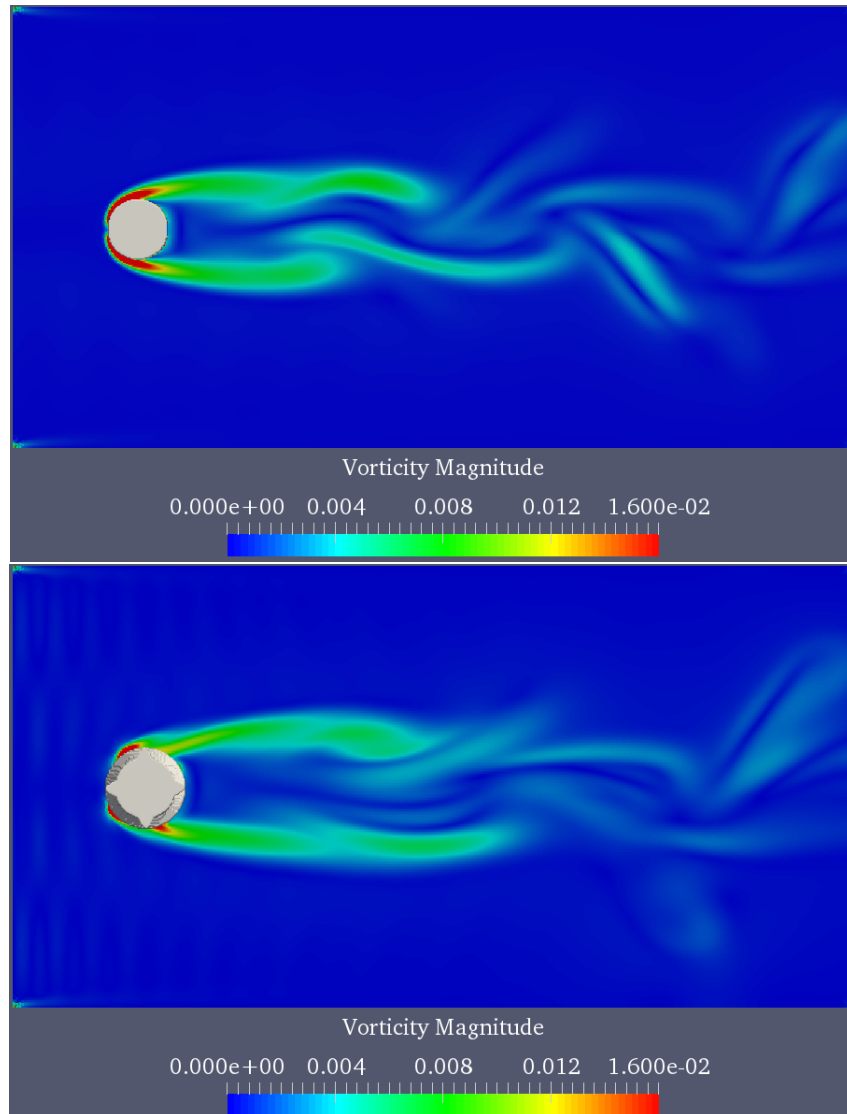


Figure 4: Vorticity for a “clean” cylinder (top) and a “decorated” one (bottom).

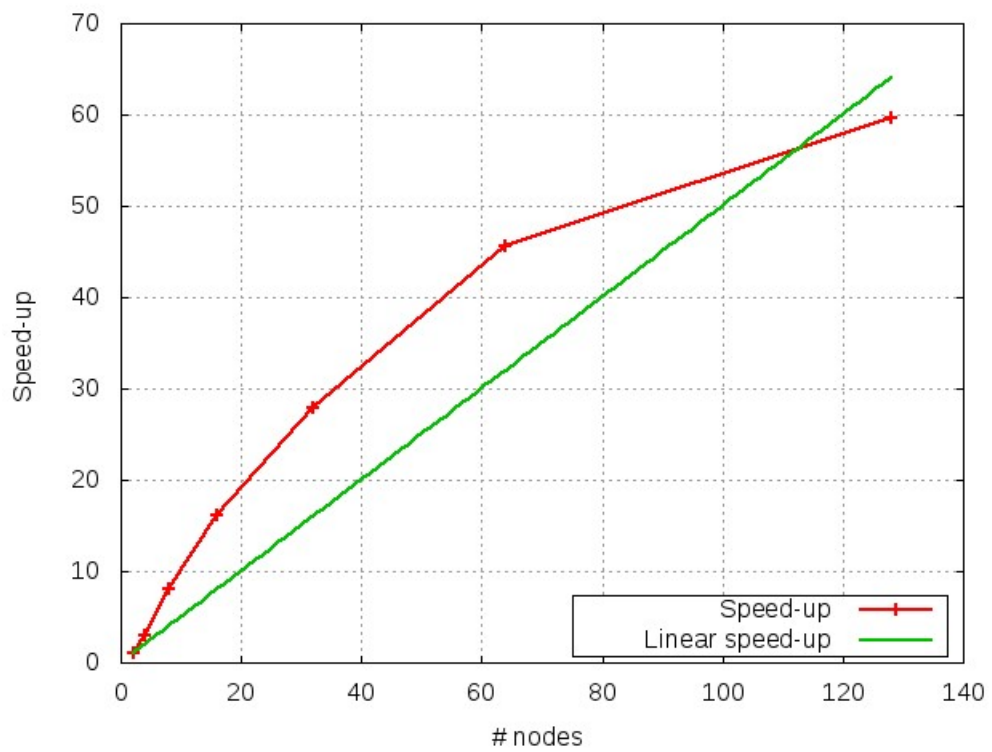


Figure 5: Strong scaling for a  $512^3$  gridpoint simulation. Note the superlinear speed-up achieved up to 128 nodes (i.e. 512 task).

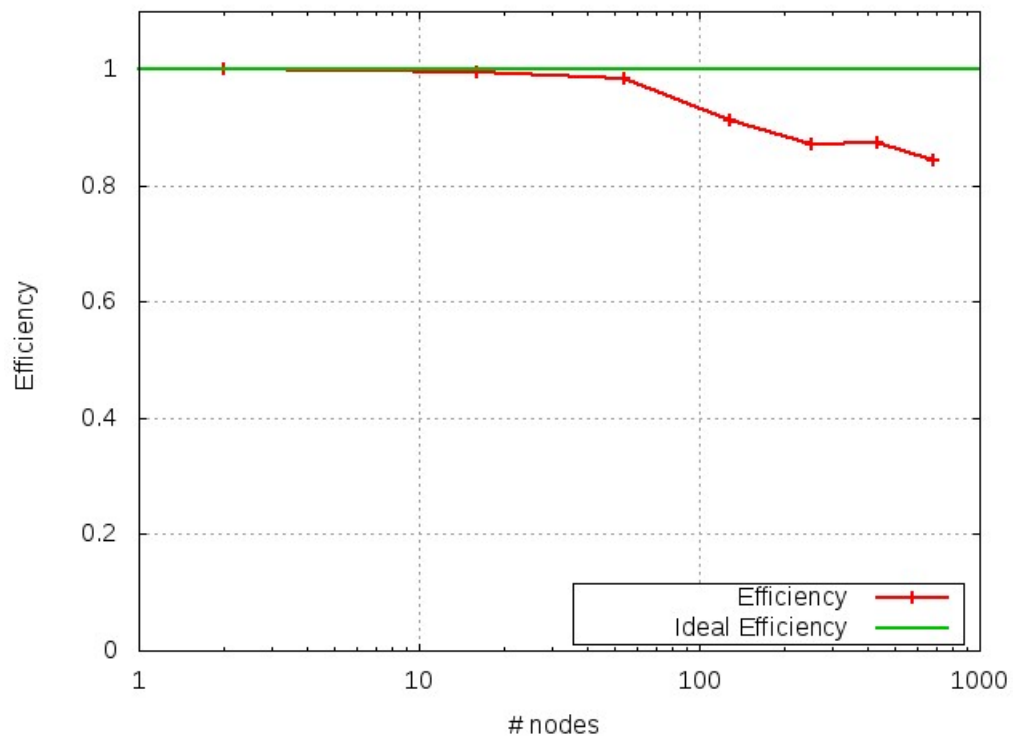


Figure 6: Weak scaling using  $128^3$  gridpoint per task. Using 2744 tasks (686 nodes) 84% of parallel efficiency is obtained.

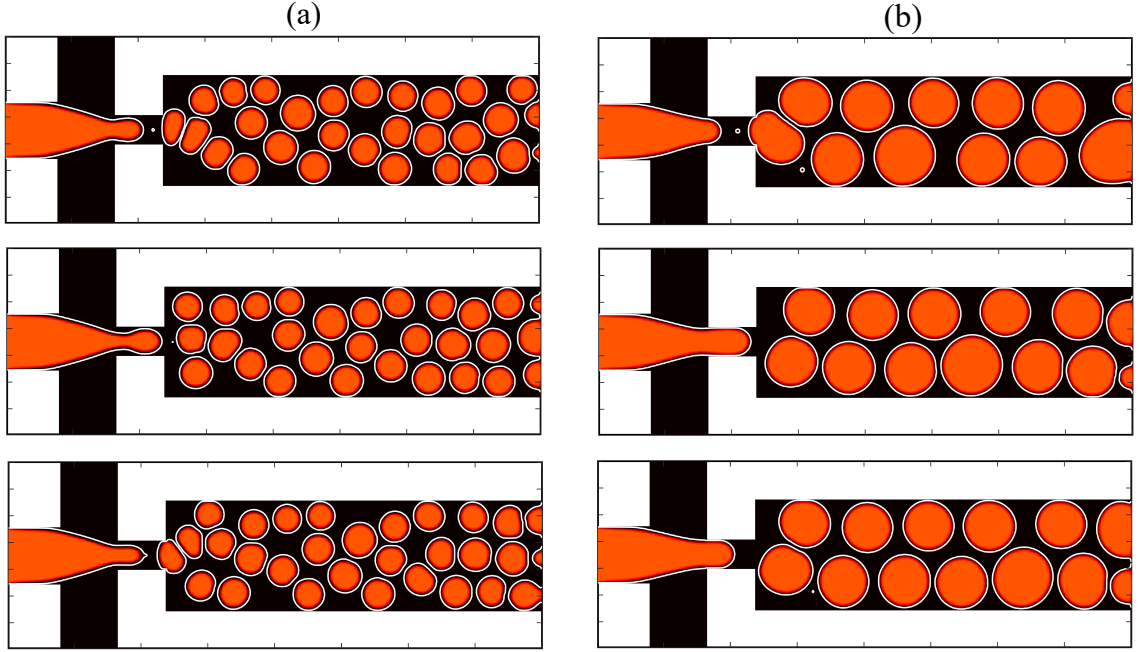


Figure 7: Different configurations of emulsions. In panel (a) the continuous to dispersed flow rate ratio  $Q_d^{in}/(2Q_c^{in}) = 2$  whereas in panel (b) is set to one. The viscosities (in lattice unit) are the same for the two fluids and set to  $\nu = 0.0167$  and the velocities of the two fluids at the inlet channels are (in lattice units/step) (a):  $u_d^{in} = 0.01$ ,  $u_c^{in} = 0.01$ , (b):  $u_d^{in} = 0.01$ ,  $u_c^{in} = 0.005$ .